BEHAVIOUR OF LIQUID TEMPERATURE AND ONSET OF NATURAL CONVECTION IN REFRIGERANT ABSORPTION IN LUBRICANT OIL

Jader R Barbosa Jr.
POLO – Research Laboratories for Emerging Technologies in Cooling and Thermophysics
Department of Mechanical Engineering, Federal University of Santa Catarina
Florianopolis, SC, 88040900, Brazil
jrb@polo.ufsc.br

Stefan M Thoma
Department of Mechanical and Process Engineering, Swiss Federal Institute of Technology
Sonneggstr. 3, 8092 Zurich, Switzerland
stthoma@student.ethz.ch

Moisés A Marcelino Neto
POLO – Research Laboratories for Emerging Technologies in Cooling and Thermophysics
Department of Mechanical Engineering, Federal University of Santa Catarina
Florianopolis, SC, 88040900, Brazil
moises@polo.ufsc.br

Abstract. *Refrigerant absorption and mixing in lubricant oil are important in the design of refrigeration compressors and refrigeration systems. Experimental work is reported on absorption of vapour R-134a through the top interface of an initially stagnant layer of pure lubricant oil. Since the liquid refrigerant is heavier than the oil, mixing is enhanced due to natural mass convection. In the present paper, the behaviour of liquid temperature during absorption is described based on measurements carried out in a test rig consisting of a transparent 77 mm ID, 150 mm long, vertical glass tube through which absorption can be directly observed. Transient liquid temperatures at three different heights in the test section (one in the vapour, two in the liquid) were measured using calibrated type-K thermocouples. The experimental work is complemented by a theoretical analysis of the critical time for the onset of mass transfer induced Rayleigh instability. The model is based on a critical mass transfer Rayleigh number criterion widely reported in the literature and takes into account the variation of physical properties in the liquid layer. The critical time for the onset of natural mass convection increases with decreasing system pressure as a result of lower equilibrium concentration at the vapour-liquid interface.*

Keywords*: Oil-refrigerant mixtures, Absorption, Rayleigh instability, Natural mass convection.*

1. INTRODUCTION

Choosing the correct working fluids for a particular refrigeration application is crucial for an efficient and reliable operation of the system and of its components. In refrigeration compressors, the thermophysical properties of the lubricant are strongly affected by the intense mixing between oil and refrigerant. For instance, because of the large difference between the viscosity of pure oil and liquid refrigerant, even small amounts of refrigerant dissolved in the oil may hamper compressor lubrication and hence reduce its life span. Another important feature of refrigerant-oil mixing is related to the determination of the equalizing pressure, i.e., the pressure attained by the system while the compressor is off. In small systems, refrigeration capacity control is performed by a succession of on-off compressor cycles. During each cycle, immediately after the compressor turns off, a process of absorption of the vapour refrigerant in the oil inside the compressor shell is initiated. In reciprocating compressors, low equalizing pressures (that depend on thermodynamic and heat and mass transport aspects of the oil and refrigerant mixture) are desirable as they mean reduced torque and less power required for compressor start-up.

Refrigerant absorption in lubricant oil has been investigated by many authors in recent years (Fukuta *et al.*, 1995; Goswami *et al.*, 1998; Yokozeki, 2002; Gessner and Barbosa, 2006). Silva (2004) conducted a series of experiments to determine the rates of absorption of R-12 in mineral oil and of R-134 in polyol ester (POE) oil. Silva measured the rates of pressure decay due to refrigerant absorption in a closed system. Experiments were performed at 15, 20 and 23^{o}C and the initial pressure of the refrigerant was of the order of 300 kPa in all cases. A 2D transient model based on mass, momentum and species conservation equations for the liquid mixture was proposed and the time-dependent refrigerant absorption was calculated taking into account the variation of height of the liquid layer. Fukuta *et al.* (2005) conducted a visualization study of R-600a absorption and desorption in oil. They measured the corresponding mass transfer rates and correlated them for conditions in which the system pressure was kept constant. Barbosa and Ortolan (2007) evaluated experimentally and theoretically absorption of R-134a and R-600a in initially pure polyol ester lubricant oils for a number of conditions in which the system pressure varied as a result of refrigerant absorption. The liquid-vapour interface temperature was measured as a function of time in some experimental runs. The temperature increase as a function of time during refrigerant absorption (latent heat release) was observed.

The first objective of the present paper is to extend the analysis of Barbosa and Ortolan (2007) by performing experiments on R-134a absorption in lubricant oil in an improved test section (with larger dimensions) in which recordings of vapour and liquid temperature were carried (in the latter, at two distances from the liquid-vapour interface). The new test section enabled a clear visualization of the liquid flow field resulting from refrigerant absorption. Depending on the refrigerant-oil pair, the liquid refrigerant is heavier than the oil and mixing is enhanced due to natural mass convection. This Rayleigh-unstable behavior is typical of HFC refrigerants, such as R-134a. In contrast, in systems where the liquid refrigerant is less dense than the oil (for example, R-600a and R-290) liquid density instability near the interface does not occur and absorption takes place by molecular diffusion alone. In unstable systems, convection is initiated by transient mass diffusion in a thin layer of liquid below the surface. The presence of an adverse density gradient near the surface (which may result from a combination of gravity and surface tension effects) gives rise to a dense layer that, once a stability limit is exceeded, plunges down as sheets and columns that evolve into inverted expanding plumes as they descend into the bulk liquid (Tan and Thorpe, 1996). A second objective of this study is to investigate theoretically the critical time for the onset of absorption induced mass convection. The model is based on the transient mass transfer Rayleigh number criterion of Tan and Thorpe (1999a) takes into account the variation of physical properties in the liquid layer. As will be shown, the critical time for the onset of convection decreases with system pressure as a result of higher equilibrium concentrations at the vapour-liquid interface. The model is compared with experimental data for absorption of R-134a in synthetic polyol ester oils.

2. EXPERIMENTS

A schematic representation of the improved experimental rig is shown in Figure 1.a (Barbosa and Ortolan, 2007). A 150 mm long section made from a 77 mm ID (~3 mm wall thickness) borosilicate glass tube is mounted between two 10 mm thick square aluminum plates. The test cell is tightened with four sets of screws and nuts (one in each corner of the plates) that press the plates against both ends of the glass tube. Silicon rubber gaskets seal the contact between the plates and the tube. Five fittings are screwed on the top plate for connecting pressure (P) and temperature (T_1, T_2, T_3) measurement devices and to allow oil and refrigerant charging (C) (see Figure 1.b).

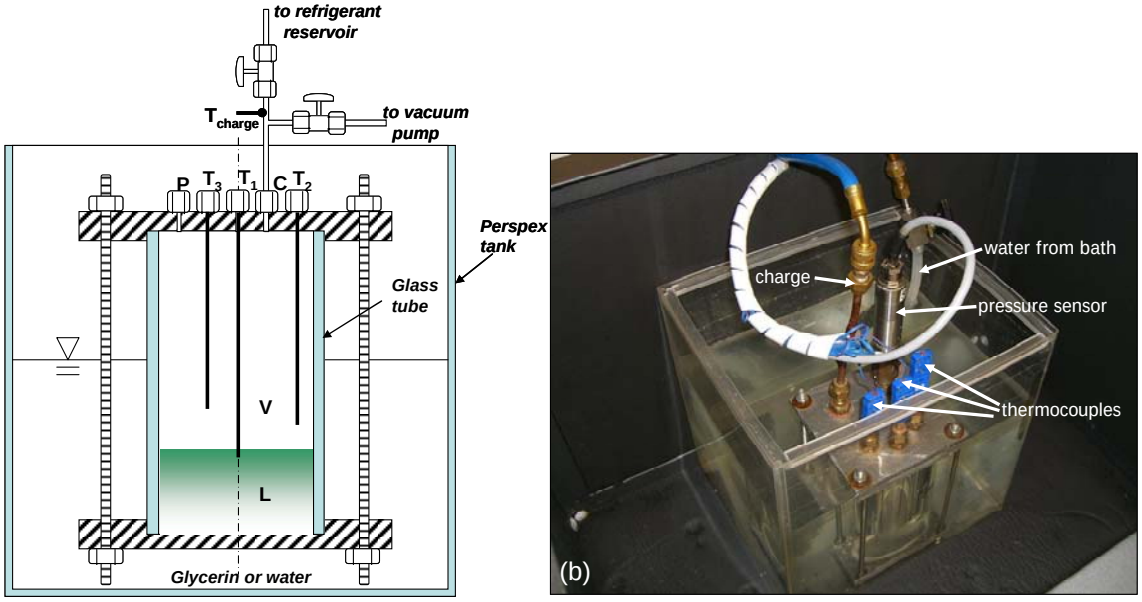

Figure 1. (a) Schematic representation of the test section. (b) Detail of connections.

Initially, a specified amount of oil (POE ISO 10) is placed inside the test cell. Vacuum is applied to the system to remove atmospheric air and moisture from the oil sample. In the temperature measurement tests, the cell is submerged into a transparent Perspex tank filled with circulation water whose temperature is controlled by a thermostatic bath (Microquimica, MQTB). In the onset of convection visualization tests, the tank is partially filled with glycerin, which has a light refraction index (1.47) very near that of borosilicate glass (approximately 1.5). In addition, any image distortion provoked by the curvature of the glass wall is cancelled out by visual observation of the flow field through the flat walls of the Perspex tank. Pressure is measured with a HBM P3MB absolute pressure transducer calibrated to an accuracy of ±0.1% of the full scale (10 bar). Temperatures of the ambient air and of the liquid mixture in the test section are measured with Omega type-K thermocouples calibrated to an accuracy of ±0.2^{o}C from 10 to 75^{o}C. The test section thermocouples are mounted in the test cell so that one of them (T_1) has only its tip is submerged in the liquid. The distances between T_1 and T_2 and between T_2 and T_3 are kept constant at 10 ± 1 mm. Time is allowed for the system to

reach thermal equilibrium with the surrounding air. The room temperature is maintained at 25 ± 0.5°C. Shortly before opening the valve that connects the test section with the refrigerant tank, the computerized data acquisition procedure is initiated.

R-134a is maintained at thermodynamic equilibrium with its liquid at room temperature inside a 500 ml reservoir. At the beginning of the test, with the valve that connects the test cell with the vacuum pump fully closed, the valve connecting the test cell and the refrigerant reservoir is carefully opened for a few seconds. This allows equalization of pressures in the reservoir and in the cell. The valve is then closed and the cell pressure decreases with time as a result of vapor refrigerant absorption in the liquid layer. The height of the liquid layer is measured with a scale on the outside of the glass tube. The experimental runs are terminated after 5 h for the R-134a runs (this time is usually enough to reach saturation). Image sequences of the absorption process were acquired with a 7Mpixel digital camera.

3. MODELLING

3.1. Absorption and Pressure Behaviour

Barbosa and Ortolan (2007) put forward a macroscopic control volume model for predicting the absorption of refrigerants in lubricant oil. Assuming that (i) the vapour behaves as an ideal gas, (ii) the system is isothermal, (iii) the vapour pressure of the oil is very low so that the vapour phase is comprised only by refrigerant and (iv) the liquid layer height variation is negligible, mass conservation in the vapour and liquid give

$$\frac{dp}{dt} = -\dot{m}_I \frac{RT}{(L_T - L)} \tag{1}$$

$$\frac{dx_R}{dt} = \frac{\dot{m}_I}{\rho_L L}(1 - x_R) \tag{2}$$

where x_R is the volume averaged refrigerant mass fraction in the liquid and L and L_T are the liquid height and the height of the test cell, respectively. The liquid density can be calculated from

$$\frac{d\rho_L}{dt} = \frac{\dot{m}_I}{L} \tag{3}$$

and the interfacial absorption mass flux is modelled in terms of a mass transfer coefficient as follows

$$\dot{m}_I = \beta(x_I - x_R) \tag{4}$$

The mass transfer coefficient is defined in terms of Sherwood and Rayleigh numbers

$$Sh = \frac{L\beta}{\rho_L \bar{\delta}_L} = C\, Ra_L^n = C\left[\frac{(x_I - x_R)\rho_L g L^3}{\bar{\eta}_L \bar{\delta}_L}\right]^n \tag{5}$$

The interfacial refrigerant mass concentration (solubility), x_I, was calculated using Raoult's law and the average liquid mass diffusivity was assumed equal to 5×10^{-10} m^2/s. Saturation pressure and pure refrigerant properties were calculated from the methods and correlations available in REFPROP 7.0 (Lemmon et al., 2002). The density and viscosity of the (pure) oils were calculated from data available from the manufacturer. The average liquid viscosity was calculated from

$$\ln(\bar{\eta}_L) = \tilde{x}_R \ln(\eta_R) + (1 - \tilde{x}_R)\ln(\eta_O) \tag{6}$$

where η_R and η_O are the viscosities of pure liquid refrigerant and oil, respectively. Equations (1)-(3) were integrated using a 4th-order Runge Kutta method (Press *et al.*, 1992). The time step was 2 s and the total integration time was 3.5×10^4 s for each run. Initial conditions were as follows: $p(t_{max}) = p_{max}$, $\rho_L(t_{max}) = \rho_O$ and $x_R(t_{max}) = 0$, where p_{max} and t_{max} are the maximum pressure in the test cell and the time at which it occurs. In the present experiments, the maximum pressure in the test section occurred at around 40 s elapsed since the valve opening.

3.2. Onset of Convection

Tan and Thorpe (1992, 1996) developed a theory for the onset of free convection in a liquid layer due to unstable transient heat conduction. As mentioned above, instability leading to convection may take place when a negative density gradient is established, such as in a layer heated from below or cooled from above. The original theory was subsequently extended (Tan and Thorpe, 1999b) to deal with the combined effect of surface tension (Marangoni convection) and density gradients and with the onset of free convection due to absorption (downward diffusion) of a heavy solute into a light solvent (Tan and Thorpe, 1999a). In this case, which is the subject of the present work, the mass transfer Rayleigh number is defined as,

$$Ra = \left(\frac{gz^4}{\eta_L \delta_L} \right) \left| \frac{\partial \rho_L}{\partial z} \right| \tag{7}$$

where g is the acceleration due to gravity, z is the downward distance measured from the liquid-vapour interface, ρ_L is the liquid mass density, η_L is the liquid absolute viscosity and δ_L is the liquid mass diffusivity. In the present study, it is assumed that the components are fully miscible and that the departure from ideal solution behaviour is small. The mixture density can thus be written as,

$$\rho_L = \left(\frac{x}{\rho_R} + \frac{1-x}{\rho_O} \right)^{-1} \tag{8}$$

where x is the local refrigerant mass fraction and the subscripts R and O stand for pure liquid refrigerant and oil, respectively. In the present stability analysis, the latent heat release at the interface as a result of absorption is neglected. It is recognized that neglecting this heat of absorption will result in an underprediction of the critical time for the onset of convection because the temperature increase associated with it reduces the mixture density near the interface.

According to Tan and Thorpe (1999a), the equivalent transient Biot number for interfacial diffusion determines whether an interface approaches the theoretical limits of Fixed Surface Concentration (FSC) ($Bi_D = \infty$) or Constant Mass Flux (CMF) ($Bi_D = 0$) boundaries. The equivalent transient Biot number may be written as

$$Bi_D = \sqrt{\frac{\delta_G}{\delta_L}} He^* \tag{9}$$

where δ is the mass diffusion coefficient and He^* is the Henry number (dimensionless Henry constant) given by

$$He^* = \frac{He}{RT} \tag{10}$$

Since the ratio between mass diffusion coefficients is of the order of 10^4 for most systems, the nature of the interfacial diffusion condition is determined by the solubility of the components (in other words, He^*). As R-134a is very soluble in POE oils, this produces a small He^* and hence a small Bi_D, which corresponds to a CMF boundary condition. It has been shown (see Tan and Thorpe, 1996, 1999a for a literature review and extensive discussions) that the value of Ra in the theoretical limits of FSC and CMF boundary conditions are 1100 and 669, respectively.

Prior to the onset of convection, the local refrigerant mass fraction is calculated assuming that absorption is due solely to diffusion in a deep fluid (a semi-infinite medium). Thus, by assuming average transport properties and solving the species conservation equation for a constant mass flux boundary condition, one has

$$x(z,t) = x_0 + \frac{2m_I''}{\rho_L} \sqrt{\frac{t}{\delta_L}}\, \mathbf{i}\mathrm{erfc}\left(\frac{z}{2\sqrt{\delta_L t}} \right) \tag{11}$$

where x_0 is the initial refrigerant mass fraction in the liquid layer (assumed equal to zero since the oil is initially pure). m_I'' is the constant interfacial mass flux, which is related to the instantaneous interfacial mass fraction by

$$x_I(t) = 2\,\mathbf{i}\mathrm{erfc}(0) \frac{m_I''}{\rho_L} \sqrt{\frac{t}{\delta_L}} \tag{12}$$

In terms of the interfacial mass fraction, Eq. (5) can be written as,

$$x(z,t) = \frac{x_I(t)}{\mathbf{i}\mathrm{erfc}(0)}\mathbf{i}\mathrm{erfc}\left(\frac{z}{2\sqrt{\delta_L t}}\right) \tag{13}$$

The maximum Rayleigh number is located at a distance $z_{\max}$ from the free surface calculated from

$$\frac{\partial}{\partial z}Ra = 0 \tag{14}$$

By substituting Eq. (7) into Eq. (14) and assuming average liquid properties one has

$$z_{\max} = -\frac{4\dfrac{\partial \rho_L}{\partial z}}{\dfrac{\partial}{\partial z}\left(\dfrac{\partial \rho_L}{\partial z}\right)} \tag{15}$$

After an algebraic manipulation of Eq. (8), the critical depth is given by

$$z_{\max} = -4\frac{\partial x}{\partial z}\left[\frac{\partial^2 x}{\partial z^2} + 2\rho_L\left(\frac{1}{\rho_O} - \frac{1}{\rho_R}\right)\left(\frac{\partial x}{\partial z}\right)^2\right]^{-1} \tag{16}$$

where

$$\frac{\partial x}{\partial z} = \frac{x_I(t)}{2\,\mathbf{i}\mathrm{erfc}(0)\sqrt{\delta_L t}}\mathrm{erfc}\left(\frac{z}{2\sqrt{\delta_L t}}\right) \tag{17}$$

$$\frac{\partial^2 x}{\partial z^2} = -\frac{x_I(t)}{2\sqrt{\pi}\,\mathbf{i}\mathrm{erfc}(0)\delta_L t}\exp\left(-\frac{z^2}{4\delta_L t}\right) \tag{18}$$

The critical mass transfer Rayleigh number is finally calculated from

$$Ra_{\mathrm{cr}} = \frac{g z_{\max}^4}{\eta_L \delta_L}\frac{\partial \rho_L}{\partial z}\bigg|_{z_{\max}} \tag{19}$$

In order to account for the significant variation of physical properties, the average liquid viscosity and mass diffusivity are calculated from (Poling *et al.*, 2000)

$$\eta_L = \frac{1}{z_P}\int_0^{z_P} \exp\left[\tilde{x}\ln\eta_R + (1-\tilde{x})\ln\eta_O\right]dz \tag{20}$$

$$\delta_L = \frac{1}{z_P}\int_0^{z_P} \delta_{OR}^{(1-\tilde{x})}\delta_{RO}^{\tilde{x}}\,dz \tag{21}$$

where z_P is the diffusion penetration depth defined as the distance at which the mass fraction becomes equal to 1% of the interfacial mass fraction. $\tilde{x}$ is the refrigerant molar fraction in the liquid phase and δ_{ij} are infinite dilution diffusion coefficients calculated from the Hayduk and Minhas correlation (Poling *et al.*, 2000).

Given that the value of the critical Rayleigh number has been established at approximately 669 for conditions similar to those of the present work, Eq. (19) is utilized to determine the critical time for the onset of convection. This is performed through a combination of the Bisection and Newton-Raphson methods (Press *et al.*, 1992), with a prescribed tolerance of 10^{-6} s.

4. RESULTS

4.1. Experimental Pressure and Temperature during Refrigerant Absorption

Experimental results on pressure decay and liquid temperature distribution are reported for R-134a/POE ISO 10 mixtures at 21, 31 and 38°C (nominal temperatures corresponding to the temperature set in the thermostatic bath). The initial height of the liquid layer (pure oil) was set at 30 mm in all cases reported here. Thus, thermocouple T_1 measures the liquid temperature approximately at the location of the interface and thermocouples T_2 and T_3 measure the vapour phase temperature at approximately 10 and 20 mm above the interface.

Figure 2 shows the pressure decay as a function of time for the experimental runs at 21, 31 and 38°C. As can be seen, the pressure initially increases as a result of refrigerant vapour release from the reservoir into the test section. The pressure then reaches a maximum and starts decreasing as refrigerant is absorbed into the lubricant oil. Eventually, as *t* becomes large, thermodynamic equilibrium will be attained and the system pressure will reach a constant value. It can be observed that the maximum pressure in the test section is approximately the same for the three temperatures. However, it is expected that less refrigerant mass enters the test cell at higher temperatures because of the lower vapour density resulting from heat transfer between the vapour and the liquid layer and the tube wall. Pressure decays more slowly at higher temperatures due to a reduction of the interfacial refrigerant mass fraction in the liquid (solubility), which also reduces the absorption driving force (difference between interfacial and bulk mass fractions – see Eq. 4).

As temperature increases within the range of the present experiments (21 to 38°C), the effect of lower interfacial mass fractions (which tends to decrease the rate of pressure decay) is stronger than the effect of the reduced initial mass of vapour (which contributes to an increase of the rate of pressure decay). Given that Eq. (1) can be written as

$$\frac{dp}{dt} = -\frac{\beta(x_I - x_R)pA}{M_{in}} \tag{22}$$

(where A is the cross sectional area of the test cell and M_{in} is the initial refrigerant mass in the vapour), one may suggest the existence of a particular point where M_{in} becomes so low (because of heat transfer to the vapour entering the cell) that it starts to dominate the rate of pressure decay. Although we have not measured the refrigerant mass entering the test cell, a thermocouple was installed on the external wall of the tubing connecting the refrigerant reservoir and the test section (see Figure 1.a) so as to provide an order of magnitude of the inlet temperature (here denoted T_{CHARGE}).

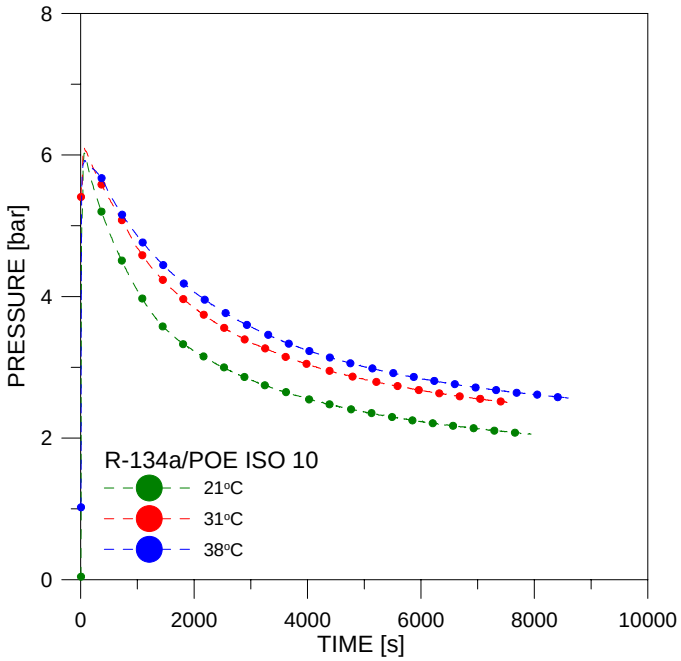

Figure 2. Pressure distribution during absorption at different temperatures.

Figures 3, 4 and 5 show the temperature distributions during the initial stages of absorption for 21, 31 and 38°C, respectively. The temperature profiles given by T_1, T_2 and T_3 show that the temperature in the vapour and liquid increases as latent heat of absorption is released at the vapour-liquid interface. It is consistently observed in the figures that, during the initial peaking period, T_3 is always less than T_2 with a time delay of a few seconds between the peaks of each distribution. These two aspects are a result of the transient nature of the heat transfer process in the vapour and are

associated with the vapour thermal capacity and 'effective' (diffusion and convection) thermal conductivity, respectively. Also shown in Figures 3-5 are the temperatures of the water in the thermostatic bath (T_{WATER}) and the temperature of the inlet tubing (T_{CHARGE}). Even at steady-state conditions, T_{WATER} is different from T_{CHARGE} because the inlet temperature sensor is not submerged and experiences heat transfer to or from the surrounding air.

It has been observed that after the initial transient temperature peaking, but for times less than 2000 to 2500 s or so, T_3 is systematically higher than T_1 and T_2. The most apparent reason for this is the lower thermal diffusivity of the vapour phase that gives rise to a time delay in the transfer of heat from the bulk vapour (whose temperature peaked during the initial stages of absorption) to the glass tube walls (whose temperature is set by the thermal bath) and to the liquid layer (that also experiences heat transfer with the tube wall, but with a much higher thermal conductance). In order to ascertain the stability and consistency of the temperature measurements, Figure 6 illustrates the temperature distributions for the whole experiment at 31°C. Eventually, T_1, T_2, T_3 and T_{WATER} become equal when absorption dies out and thermal equilibrium is achieved.

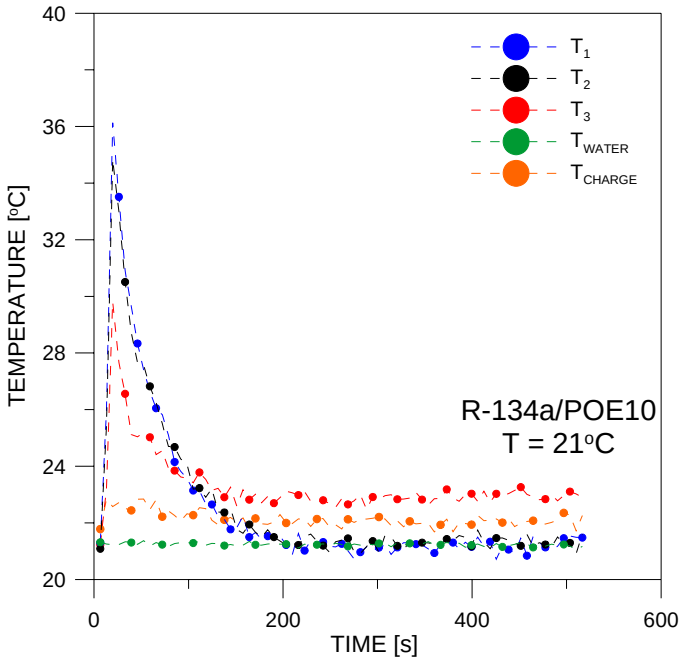

Figure 3. Temperature distribution during absorption at 21°C (nominal).

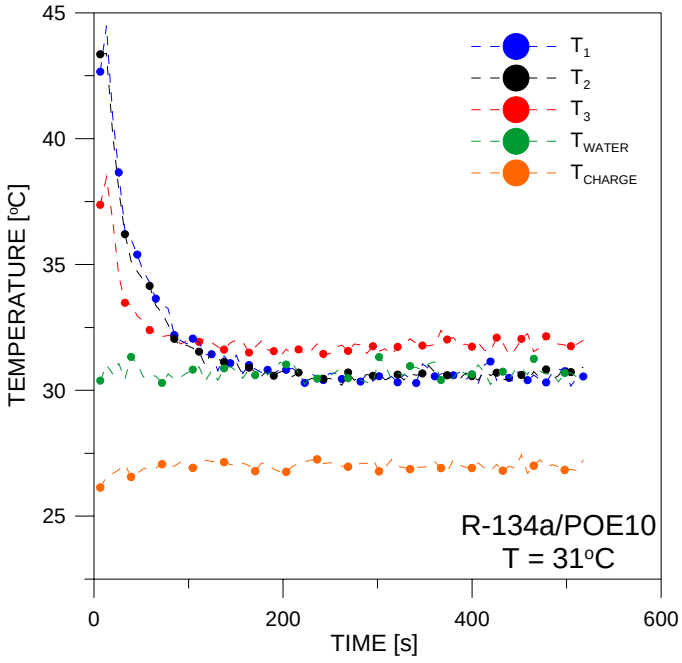

Figure 4. Temperature distribution during absorption at 31°C (nominal).

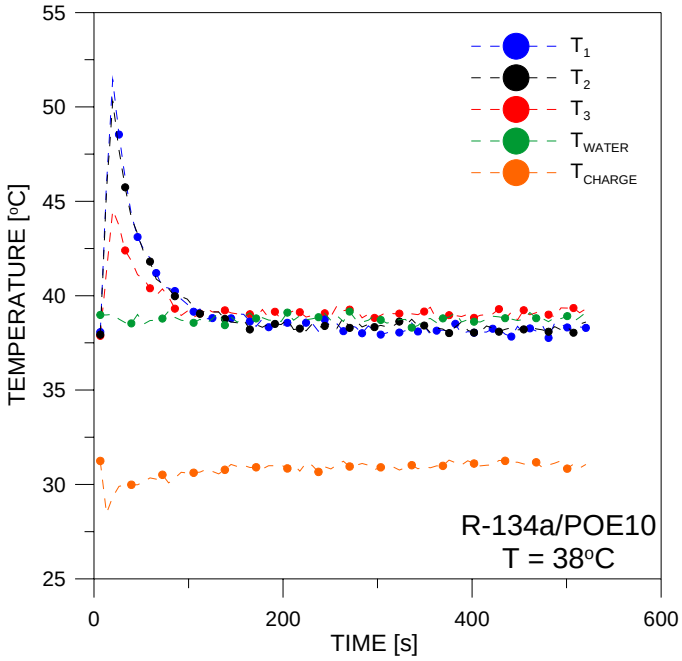

Figure 5. Temperature distribution during absorption at 38°C (nominal).

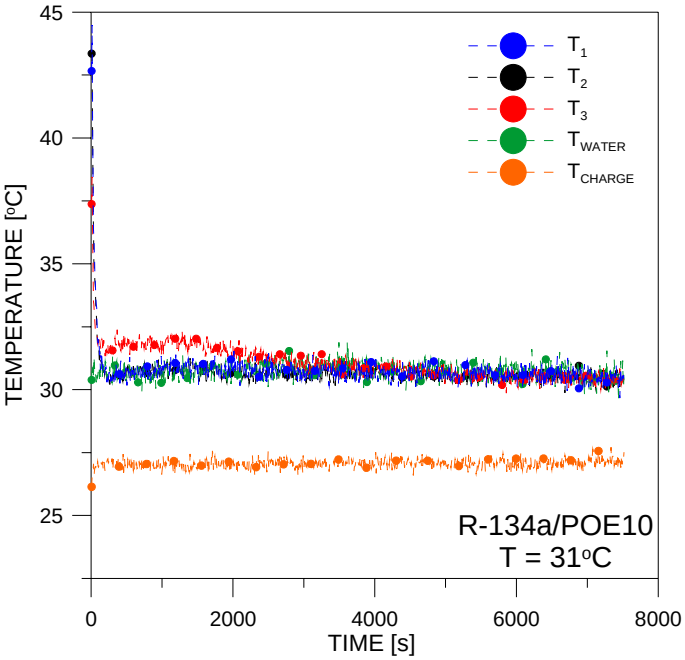

Figure 6. Temperature distribution during absorption at 31°C (nominal).

4.2. Visualization

Figure 7 shows a visualization run for a condition in which the system was maintained at ambient temperature and the initial pressure corresponded to approximately 95% of the saturation pressure of the refrigerant at the ambient temperature. The time elapsed since the first frame is shown for each frame. As can be seen, absorption appears to begin with a disturbance of the interface, just as described qualitatively by Tan and Thorpe (1996, 1999a). The disturbances then evolve into descending inverted plumes that are a typical feature of natural mass convection.

4.3. Predictions of Pressure during Absorption

Figure 8 shows the predictions of pressure as a function of time during absorption of vapour R-134a in POE ISO 10 at 21, 31 and 38°C. The pressure has been normalized with respect to the maximum pressure at each run. As in Barbosa

and Ortolan (2007), reasonable agreement with the experimental data was observed when the average liquid mass diffusivity was set at 5×10^{-10} m^2/s. The values of C and n in Equation (5) were set at 0.27 and 0.25, respectively. As can be seen from the figure, the agreement between the model predictions and the experimental data is good at 21^{o}C but, as the temperature increases, the model overpedicts the experimental data.

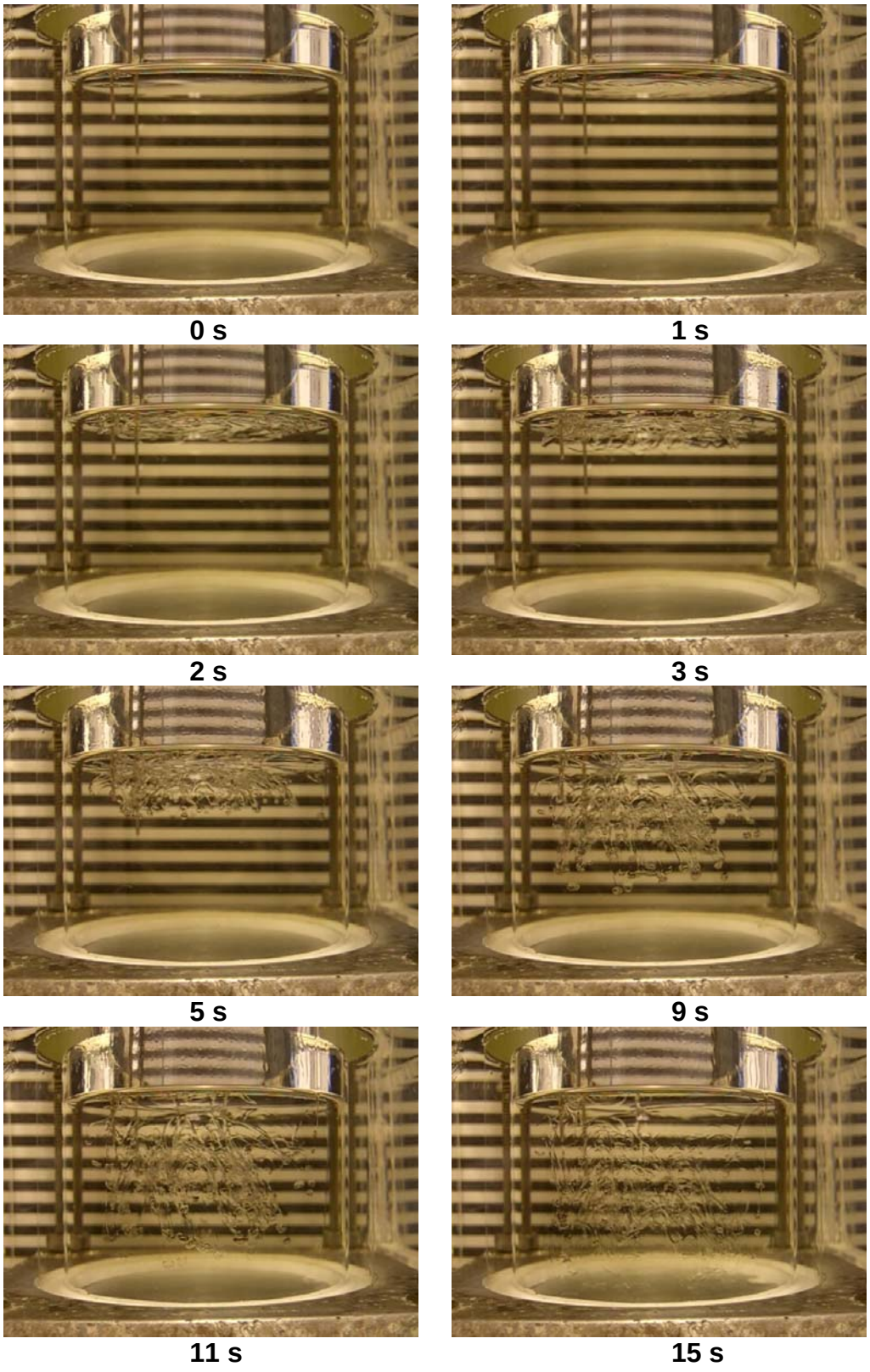

Figure 7. Visualization of absorption of R-134a in POE ISO 10 oil.

There are several mechanisms which may be responsible for the observed deviations between predictions and experimental results. Firstly, for simplicity, the system is assumed to behave isothermally. As was shown above, this is not true especially during the first stages of the absorption process. In addition to modifying the physical properties (density and viscosity), a variation of the interface temperature would also affect the Vapour-Liquid Equilibrium (VLE) behaviour. Secondly, in the present experiments, there is sensible heat transfer between the liquid and the vapour (they are initially brought together at different temperatures) and between the liquid and vapour and the surroundings (circulation water). This effect was not included in the model and is expected to increase of the rates of absorption because solubility (i.e., the interfacial concentration) increases with decreasing temperature. Thirdly, ideal mixture behaviour is assumed and VLE is calculated using Raoult's Law. Finally, physical properties (density, viscosity and mass diffusivity) were calculated in a simplified manner in all cases. Compounded together, these simplifications surely have some effect on the performance of the present formulation and shall be dealt with in greater detail in future developments of the model for mixtures involving R-134a and other refrigerants.

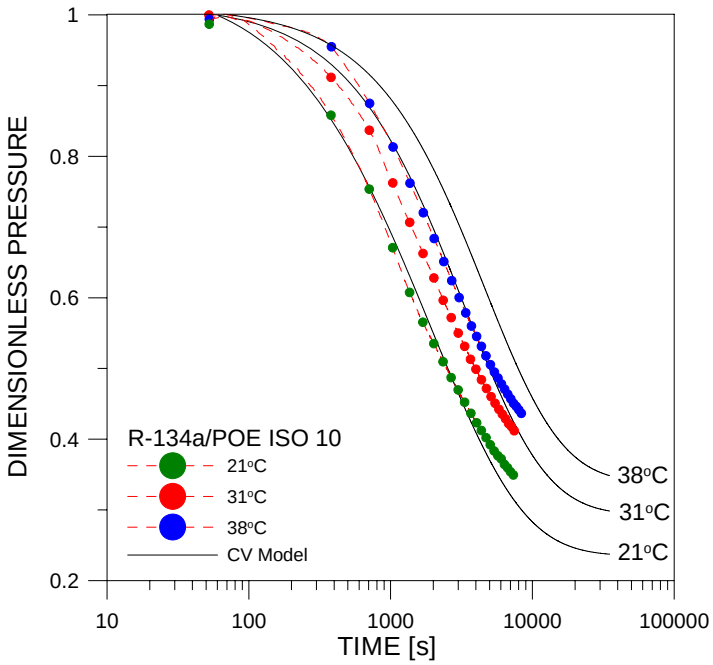

Figure 8. Predictions of pressure decay as a function of time for R-134a in POE ISO 10 oil.

4.4. Predictions of the Onset of Convection

The model described in Section 3.2 was applied in the prediction of the onset of convection in refrigerant absorption in oil. Figures 9 and 10 show the calculated critical time for the onset of natural mass convection as a function of system temperature and pressure for absorption of R-134a in oils POE ISO 7 (a lubricant of the same type as that investigated here but of a lower viscosity grade) and POE ISO 10, respectively. The critical times, in general, are higher for POE ISO 10 (more viscous) than for POE ISO 7. At a given temperature, the lowest critical time corresponds to the condition where the initial system pressure is equal to the refrigerant saturation pressure. When pressure decreases at a constant temperature, the critical time for the onset of convection increases. This is a result of the associated reduction of mass transfer driving force, i.e. the difference between the interfacial and bulk refrigerant mass fractions, from a value equal to unity (when the system pressure is equal to the saturation pressure) to values less than that as the system pressure decreases. At a constant pressure, the critical time also increases with temperature because the solubility (interfacial mass fraction) is inversely proportional to the temperature.

Barbosa and Ortolan (2007) estimated the critical time for the onset of convection in R-134a/POE ISO 7 and R-134a/POE ISO 10 mixtures. The measurement was based on visual assessment of video sequences obtained for tests carried out at 25 ± 0.5 ^{o}C in which the maximum pressure in the test section was approximately equal to 95% of the saturation pressure of the refrigerant at the ambient temperature. In the present work, the onset of convection was measured at two conditions for R-134a/POE ISO 10. In the first, the maximum pressure was also approximately equal to 95% of the saturation pressure of the refrigerant at the ambient temperature (25 ± 0.5 ^{o}C). In the second case, the maximum pressure in the test section was set at approximately 61% of the saturation pressure of the refrigerant at the ambient temperature by having a lower mass of refrigerant vapour in the reservoir at the beginning of the experiment.

Table 1 shows a comparison between the measured and predicted critical times for the onset of convection in the present experiments and those of Barbosa and Ortolan (2007). As can be seen, the agreement between the model and the experiments of Barbosa and Ortolan (2007) is quite satisfactory. However, the agreement between the model and the present experiments is only good for one condition. A possible reason for the observed discrepancy may be related to the different manner with which the valve was open to release the gas from the reservoir into the test cell. In the experiments of Barbosa and Ortolan (2007), the valve was opened more abruptly and kept open for shorter intervals. In the present work, several seconds elapsed between the start of the valve opening (which was slow but continuous) and the point of maximum test section pressure (see abscissa of Figure 8), which preceded by a few seconds the instant of valve closure. This caused the average test section pressure prior to the onset of absorption to be less than the maximum pressure and reduced the driving force for refrigerant absorption in comparison with a situation where the maximum pressure is attained within a few seconds from the valve opening.

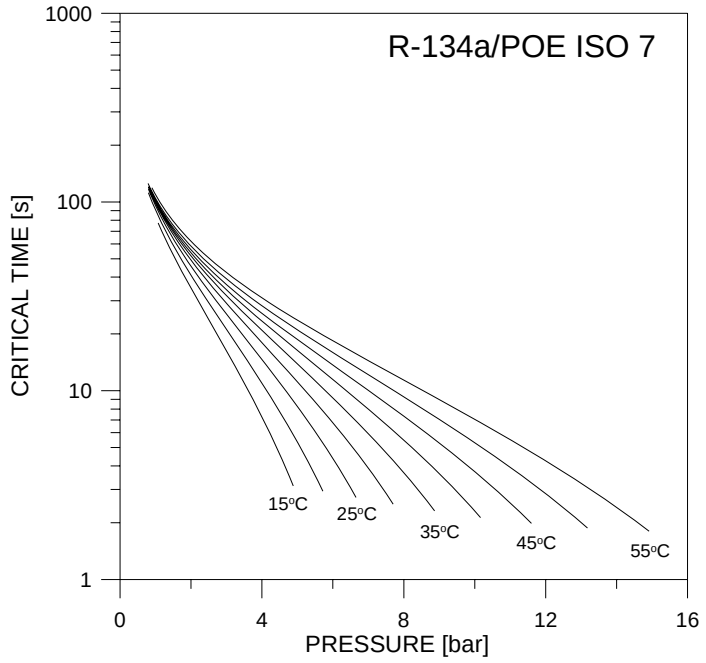

Figure 9. Predictions of critical time for absorption of R-134a in POE ISO 7.

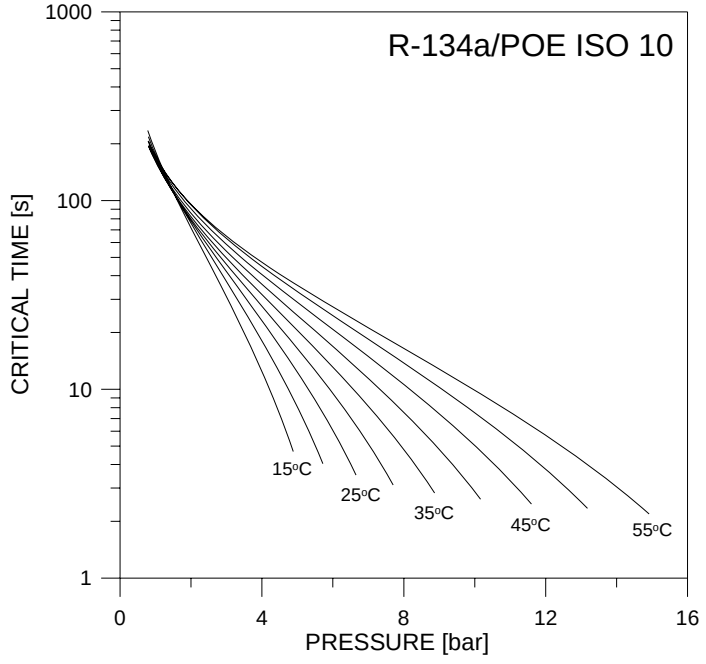

Figure 10. Predictions of critical time for absorption of R-134a in POE ISO 10.

Table 1. Comparison of experimental and predicted critical times for the onset of convection.

Experiment	Measured t_{crit}	Predicted t_{crit}
R-134a/POE ISO 7[(1)]	2 ± 1 s	3.49
R-134a/POE ISO 10[(1)]	5 ± 1 s	4.94
R-134a/POE ISO 10[(2)]	10 ± 1 s	4.94
R-134a/POE ISO 10[(3)]	25 ± 1 s	23.21

(1) : Barbosa and Ortolan (2007); (2) : This work, $p_{max} = 0.95\, p_{sat}$; (3) : This work, $p_{max} = 0.61\, p_{sat}$

5. CONCLUSIONS

This paper presented a study on flow field visualization and experimental assessment of absorption of vapour R-134a in polyol ester (POE ISO 10) lubricant oil. While the absorption of some refrigerants is controlled solely by diffusion, the R-134a/POE system is Rayleigh unstable and the resulting flow field during absorption is due to natural mass convection.

Liquid temperature and system pressure as a function of time were acquired for 21, 31 and 38°C (nominal). The temperature rise of the liquid associated with the latent heat release was recorded during selected runs. Two mathematical models were implemented to predict the pressure decay and during absorption and the critical time associated with the onset of natural mass convection. Despite the many assumptions involved in both analyses, the agreement of the models with the experimental data is very encouraging.

6. ACKNOWLEDGEMENTS

This work was financially supported by Embraco. The authors thank Alexandre Pereira and Fabiano Vambommel for technical assistance.

7. REFERENCES

Barbosa, Jr., J.R. and Ortolan, M.A., 2007, "Experimental and Theoretical Analysis of Refrigerant Absorption in Lubricant Oil", in press, HVAC&R Research.

Fukuta, M., Yanagizawa, T., Shimizu, T. and Nishijima, H., 1995, "Transient Mixing Characteristics of Refrigerant with Refrigeration Oil", Proc.19th Int. Congress of Refrigeration IVa, 215-222.

Fukuta, M., Yanagisawa, T., Omura, M. and Ogi, Y., 2005, "Mixing and Separation Characteristics of Iso-butane with Refrigeration Oil", Int. J. Refrig., 28, 997-1005.

Gessner, T.R. and Barbosa Jr., J.R., 2006, "Modeling Absorption of Pure Refrigerants and Refrigerant Mixtures In Lubricant Oil", International Journal of Refrigeration, 29, 773-780.

Goswami, D.Y., Shah, D.O., Jotshi, C.K., Bhagwat, S.S., Leung, M., Gregory, A.S. and Lu S., 1998, "Foaming Characteristics of of Refrigerant/Lubricant Mixtures", ARTI-MCLR Report 665-53200.

Lemmon, E.W., McLinden, M.O. and Huber, M.L., 2002, REFPROP v.7.0, NIST Standard Reference Database 23, NIST, USA.

Poling, B.E., Prausnitz, J.M. and O'Connell, J.P., 2000, "The Properties of Gases and Liquids", 5th Ed. Mc-Graw-Hill.

Press, W.H., Teukolsky, S.A., Vetterling, W.T. and Flannery, B.P., 1992, "Numerical Recipes in FORTRAN – The Art of Scientic Computing", Cambridge University Press, 2nd Edition.

Silva, A., 2004, "Cinemática e Dinâmica do Processo de Absorção de Gás Refrigerante em Óleo Lubrificante", Tese de Doutorado, Universidade Federal de Santa Catarina.

Tan, K.K. and Thorpe, R.B., 1992, "Gas Diffusion into Viscous and non-Newtonian Liquids", Chem. Eng. Sci., 47, 3565-3572.

Tan, K.K. and Thorpe, R.B., 1996, "The Onset of Convection Caused by Buoyancy during Transient Heat Conduction in Deep Fluids", Chem. Eng. Sci., 51, 4127-4136.

Tan, K.K. and Thorpe, R.B., 1999a, "The Onset of Convection Induced by Buoyancy during Gas Diffusion in Deep Fluids", Chem. Eng. Sci., 54, 4179-4187.

Tan, K.K. and Thorpe, R.B., 1999b, "On convection driven by surface tension caused by transient heat conduction", Chem. Eng. Sci., 54, 775-783.

Yokozeki, A., 2002, "Time-Dependent Behavior of Gas Absorption in Lubricant Oil", International Journal of Refrigeration, 25, 695-704.